Physics in Collision - Zeuthen, Germany, June 26-28, 2003

Observation of New Narrow D_s states

Antimo Palano
from the BABAR Collaboration
INFN and University of Bari, Italy

ABSTRACT

The *BABAR* experiment has discovered a new narrow state, $D^*_{sJ}(2317)^+$, near 2.32 GeV/c^2 in the inclusive $D_s^+\pi^0$ invariant mass distribution from e^+e^- annihilation data at energies near 10.6 GeV [1]. The same experiment has also shown evidence for structure in the 2.46 GeV/c^2 region in the $D_s^*(2112)^+\pi^0$ mass spectrum. These discoveries have triggered several experiments in a search for new states coupled to the D_s^+ meson which confirmed the existence of $D^*_{sJ}(2317)^+$ together with $D_{sJ}(2458)^+ \to D_s^*(2112)^+\pi^0$ both in inclusive e^+e^- annihilation and in B decays. These two new states are difficult to explain in terms of potential models.

1 Introduction

Experimental information on the spectrum of the $c\overline{s}$ meson states is limited. The $^1S_0$ ground state, the D_s^+ meson, is well-established, as is the $^3S_1$ ground state, the $D_s^*(2112)^+$. Only two other $c\overline{s}$ states are listed in the last PDG edition [2]. The $D_{s1}(2536)^+$ has been detected in its D^*K decay mode and analysis of the D^* decay angular distribution prefers $J^P = 1^+$. The $D_{sJ}^*(2573)^+$ was discovered in its D^0K^+ decay mode and so has natural spin-parity. The assignment $J^P = 2^+$ is consistent with the data, but is not established.

The spectroscopy of $c\overline{s}$ states is simple in the limit of large charm-quark mass [3, 4]. In that limit, the total angular momentum $\vec{j} = \vec{l} + \vec{s}$ of the light quark, obtained by summing its orbital and spin angular momenta, is conserved. The P-wave states, all of which have positive parity, then have $j = 3/2$ or $j = 1/2$. Combined with the spin of the heavy quark, the former gives total angular momentum $J = 2$ and $J = 1$, while the latter gives $J = 1$ and $J = 0$. The $J^P = 2^+$ and $J^P = 1^+$ members of the $j = 3/2$ doublet are expected to have small width [5], and are identified with the $D_{sJ}^*(2573)^+$ and $D_{s1}(2536)^+$, respectively, although the latter may include a small admixture of the $j = 1/2$, $J^P = 1^+$ state. Theoretical models typically predict masses between 2.4 and 2.6 GeV/c^2 for the remaining two states [6, 5, 7], both of which should decay by kaon emission. They would be expected to have large widths [5, 7] and hence should be difficult to detect.

The experimental and theoretical status of the P-wave $c\overline{s}$ states thus can be summarized by stating that experiment has provided good candidates for the two states that theory predicts should be readily observable, but has no candidates for the two states that should be difficult to observe because of their large predicted widths.

2 The *BABAR* Experiment.

The *BABAR* detector (at the PEP-II asymmetric-energy e^+e^- storage ring with center-of-mass energy near 10.6 GeV) is a general purpose, solenoidal, magnetic spectrometer and is described in detail elsewhere [8]. The data sample use in this analysis corresponds to an integrated luminosity of 91 fb^{-1}.

3 $D_s^+\pi^0$ events selection.

The objective of this analysis is to investigate the inclusively-produced $D_s^+\pi^0$ mass spectrum by combining charged particles corresponding to the decay $D_s^+ \to K^+K^-\pi^+$ [1] with π^0 candidates reconstructed from a pair of photons and performing a one-constraint fit to the π^0 mass. A given event may yield several acceptable π^0 candidates retaining only those candidates for which neither photon belongs to another acceptable π^0 candidate. To reduce combinatorial background from the continuum and eliminate background from B-meson decay, each $K^+K^-\pi^+\pi^0$ candidate was required to have a center-of-mass momentum p^* greater than 2.5 GeV/c.

The upper histogram in Fig. 1(a) shows the $K^+K^-\pi^+$ mass distribution for all candidates. Clear peaks corresponding to D^+ and D_s^+ mesons are seen. To reduce the background further, only those candidates with K^+K^- mass within 10 MeV/c^2 of the $\phi(1020)$ mass or with $K^-\pi^+$ mass within 50 MeV/c^2 of the $\overline{K}^*(892)$ mass are retained. The decay products of the vector particles $\phi(1020)$ and $\overline{K}^*(892)$ exhibit the expected $\cos^2\theta_h$ behavior required by conservation of angular momentum, where θ_h is the helicity angle. The signal-to-background ratio is further improved by requiring $|\cos\theta_h| > 0.5$. The lower histogram of Fig. 1(a) shows the net effect of these additional selection criteria. The D_s^+ signal and sideband regions are shaded. The D_s^+ signal peak, consisting of approximately 80,000 events, is centered at a mass of (1967.20 ± 0.03) MeV/c^2 (statistical error only).

Figure 1(b) shows the mass distribution for all two-photon combinations associated with the selected events. The π^0 signal and sideband regions are shaded. Candidates in the D_s^+ signal region of Fig. 1(a) are combined with the mass-constrained π^0 candidates to yield the mass distribution of Fig. 1(c). A clear, narrow signal at a mass near 2.32 GeV/c^2 is seen. The shaded histogram represents the events in the $D_s^+ \to K^+K^-\pi^+$ mass sidebands combined with the π^0 candidates. In Fig. 1(d) the mass distributions result from the combination of the D_s^+ candidates with the photon pairs from the π^0 signal and sideband regions of Fig. 1(b) (the sideband distribution is again shaded). In Figs. 1(c) and 1(d) the 2.32 GeV/c^2 signal is absent from the sideband distributions indicating quite clearly that the peak is associated with the $D_s^+\pi^0$ system. In order to improve mass resolution, the nominal D_s^+ mass [2] has been used to calculate the D_s^+ energy.

The $D_s^+\pi^0$ mass distribution for $p^*(D_s^+\pi^0) > 3.5$ GeV/c is shown in Fig. 2(a). The fit function drawn on Fig. 2(a) comprises a Gaussian function describing the 2.32 GeV/c^2 signal and a polynomial background distribution function. The fit

[1] The inclusion of charge-conjugate configurations is implied throughout this paper.

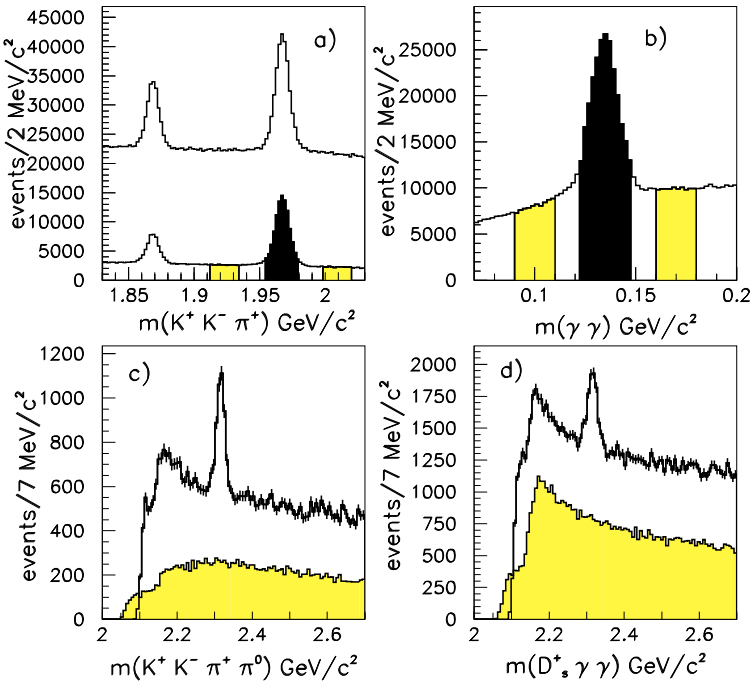

Figure 1: *BABAR* experiment. (a) The distribution of $K^+K^-\pi^+$ mass for all candidate events. Additional selection criteria have been used to produce the lower histogram. (b) The two-photon mass distribution from $D_s^+\pi^0$ candidate events. D_s^+ and π^0 signal and sideband regions are shaded. (c) The $D_s^+\pi^0$ mass distribution for candidates in the D_s^+ signal (top histogram) and $K^+K^-\pi^+$ sideband regions (shaded histogram) of (a). (d) The $D_s^+\gamma\gamma$ mass distribution for signal D_s^+ candidates and a photon pair from the π^0 signal region of (b) (top histogram) and the sideband regions of (b) (shaded histogram).

yields 1267 ± 53 candidates in the signal Gaussian with mass (2316.8 ± 0.4) MeV/c^2 and standard deviation (8.6 ± 0.4) MeV/c^2 (statistical errors only). The signal, labelled as $D_{sJ}^*(2317)^+$, is observed in both the $\phi\pi^+$ and $\overline{K}^{*0}K^+$ decay modes of the D_s^+. In addition, a sample of $D_s^+ \to K^+K^-\pi^+\pi^0$ decays is selected by adding π^0 candidates to each $K^+K^-\pi^+$ candidate. Each resulting D_s^+ candidate is combined with a second π^0 candidate with lab momentum greater than 300 MeV/c. A clear $D_{sJ}^*(2317)^+$ signal is observed as shown in Fig. 2(b). A Gaussian fit yields 273 ± 33 events with a mean of (2317.6 ± 1.3) MeV/c^2 and width (8.8 ± 1.1) MeV/c^2 (statistical errors only). The mean and width are consistent with the values obtained for the $D_s^+ \to K^+K^-\pi^+$ decay mode. The mass distribution of the $D_s^+ \to K^+K^-\pi^+\pi^0$ sample (not shown) peaks at (1967.4 ± 0.2) MeV/c^2 (statistical error only).

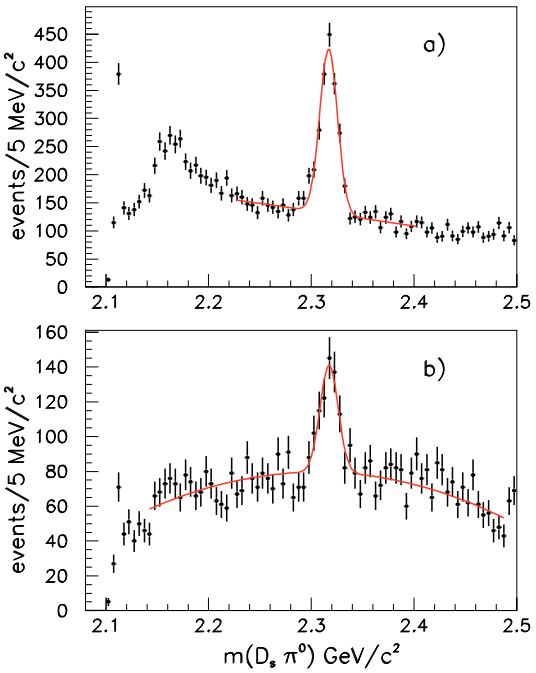

Figure 2: *BABAR* experiment. The $D_s^+\pi^0$ mass distribution for (a) the decay $D_s^+ \to K^+K^-\pi^+$ and (b) the decay $D_s^+ \to K^+K^-\pi^+\pi^0$.

Monte Carlo simulations have been used to investigate the possibility that the $D_{sJ}^*(2317)^+$ signal could be due to reflection from other charmed states. This simulation includes $e^+e^- \to c\bar{c}$ events and all known charm states and decays. The generated events were processed by a detailed detector simulation and subjected to the same reconstruction and event-selection procedure as that used for the data. No peak is found in the 2.32 GeV/c^2 $D_s^+\pi^0$ signal region.

Mass resolution estimates for the $K^+K^-\pi^+\pi^0$ system are obtained directly from the data using a fit to the mass distribution $D_s^+ \to K^+K^-\pi^+\pi^0$. The measured width from this mode is consistent with that of the $D_{sJ}^*(2317)^+$ signal. It can be concluded that the intrinsic width of the $D_{sJ}^*(2317)^+$ is small ($\Gamma \lesssim 10$ MeV).

A search has also been performed for the decay $D_{sJ}^*(2317)^+ \to D_s^+\gamma$. Shown in Fig. 3(a) is the $D_s^+\gamma$ mass distribution obtained by combining a D_s^+ candidate in the signal region of Fig. 1(a) with a photon with an energy of at least 150 MeV that does not belong to a $\gamma\gamma$ combination in the signal region of Fig. 1(b). The requirement that the p^* of the $D_s^+\gamma$ system be greater than 3.5 GeV/c is also imposed. There is a clear $D_s^*(2112)^+$ signal, but no indication of $D_{sJ}^*(2317)^+$ production. The

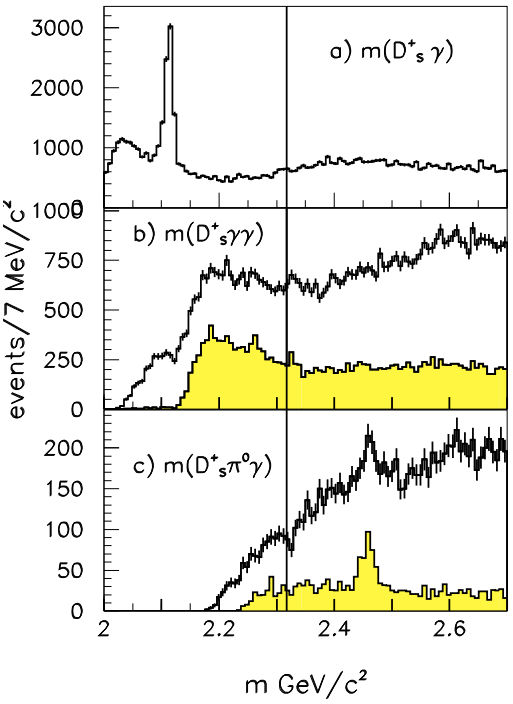

Figure 3: *BABAR* experiment. The mass distribution for (a) $D_s^+\gamma$ and (b) $D_s^+\gamma\gamma$ after excluding photons from the signal region of Fig. 1(b). (c) The $D_s^+\pi^0\gamma$ mass distribution. The lower histograms of (b) and (c) correspond to $D_s^+\gamma$ masses that fall in the $D_s^*(2112)^+$ signal region as described in the text. The vertical line indicates the $D_{sJ}^*(2317)^+$ mass.

$D_s^+\gamma\gamma$ mass distribution for $p^*(D_s^+\gamma\gamma) > 3.5$ GeV/c, excluding any photon that belongs to the π^0 signal region of Fig. 1(b), is shown as the upper histogram of Fig. 3(b). No signal is observed near 2.32 GeV/c^2. The shaded histogram corresponds to the subset of combinations for which either $D_s^+\gamma$ combination lies in the $D_s^*(2112)^+$ region, defined as $2.096 < m(D_s^+\gamma) < 2.128$ GeV/c^2. Again, no $D_{sJ}^*(2317)^+$ signal is evident, thus demonstrating the absence of a $D_s^*(2112)^+\gamma$ decay mode at the present level of statistics. The $D_s^+\pi^0\gamma$ mass distribution, excluding any photon that belongs to any π^0 candidate, is shown as the upper histogram of Fig. 3(c). The shaded histogram corresponds to the subset of combinations in which the $D_s^+\gamma$ mass falls in the $D_s^*(2112)^+$ region. No signal is observed near 2.32 GeV/c^2 in either case. A small peak, however, is visible near a mass of 2.46 GeV/c^2. This mass corresponds to the overlap region of the $D_s^*(2112)^+ \to D_s^+\gamma$ and $D_{sJ}^*(2317)^+ \to D_s^+\pi^0$ signal bands

that, because of the small widths of both the $D_s^*(2112)^+$ and $D_{sJ}^*(2317)^+$ mesons, produces a narrow peak in the $D_s^+\pi^0\gamma$ mass distribution that survives a $D_s^*(2112)^+$ selection.

If the peak in the $D_s^+\pi^0\gamma$ mass distribution of Fig. 3(c) were due to the production of a narrow state with mass near 2.46 GeV/c^2 decaying to $D_s^*(2112)^+\pi^0$, the kinematics are such that a peak would be produced in the $D_s^+\pi^0$ mass distribution at a mass near 2.32 GeV/c^2. Such a $D_s^+\pi^0$ mass peak, however, would have a root-mean-square of ~ 15 MeV/c^2, which is significantly larger than that obtained for the $D_{sJ}^*(2317)^+$ signal. In addition, Monte Carlo studies indicate that if the apparent signal at 2.46 GeV/c^2 were due to a state that decays entirely to $D_s^*(2112)^+\pi^0$, it would produce only one-sixth of the observed signal at 2.32 GeV/c^2.

The *BABAR* experiment was somewhat coutious in claiming the discovery of this second state. "Although we rule out the decay of a state of mass 2.46 GeV/c^2 as the sole source of the $D_s^+\pi^0$ mass peak corresponding to the $D_{sJ}^*(2317)^+$, such a state may be produced in addition to the $D_{sJ}^*(2317)^+$. However, the complexity of the overlapping kinematics of the $D_s^*(2112)^+ \to D_s^+\gamma$ and $D_{sJ}^*(2317)^+ \to D_s^+\pi^0$ decays requires more detailed study, currently underway, in order to arrive at a definitive conclusion [1]."

4 Confirmation of $D_{sJ}^*(2317)^+$ and observation of $D_{sJ}(2458)^+$ by other experiments.

Using 13.5 and 78 fb^{-1} integrated luminosity, the CLEO [9] and Belle [11] experiments readily confirmed the existence of $D_{sJ}^*(2317)^+$ (shown in fig 4). In terms of $\Delta m = m(K^+K^-\pi^+\pi^0) - m(K^+K^-\pi^+)$, CLEO reported a value of $\Delta m = 350.3 \pm 1.0$ MeV/c^2 with 231 $\pm$ 30 events. Belle reports $\Delta m = 348.9 \pm 0.5$ MeV/c^2 with 643 $\pm$ 50 events. These values are in good agreement with the *BABAR* measurement of $\Delta m = 384.4 \pm 0.4$ MeV/c^2.

In addition, both the CLEO and Belle Collaborations have analyzed the $D_s^*(2112)^+\pi^0$ mass distribution finding evidence for structure in the 2.46 GeV region (see fig. 5). Defining now $\Delta m = m(K^+K^-\pi^+\pi^0\gamma) - m(K^+K^-\pi^+\gamma)$, they reported the following parameters for this state: Δm=351.2 $\pm$ 1.7 MeV/c^2 with 41$\pm$12 events (CLEO) and Δm=344.1 $\pm$ 1.3 MeV/c^2 with 79 $\pm$ 18 events (Belle).

Belle also reported evidence for both states [10] in the B decays to $B \to DD_{sJ}^*(2317)^+$ and $B \to DD_{sJ}(2458)^+$. In addition, they reported an observation of $D_{sJ}(2458)^+ \to D_s^+\gamma$ in both B decays and continuum e^+e^- annihilations. The angular analysis shows the expected behaviour for a $J^P = 1^+$ state.

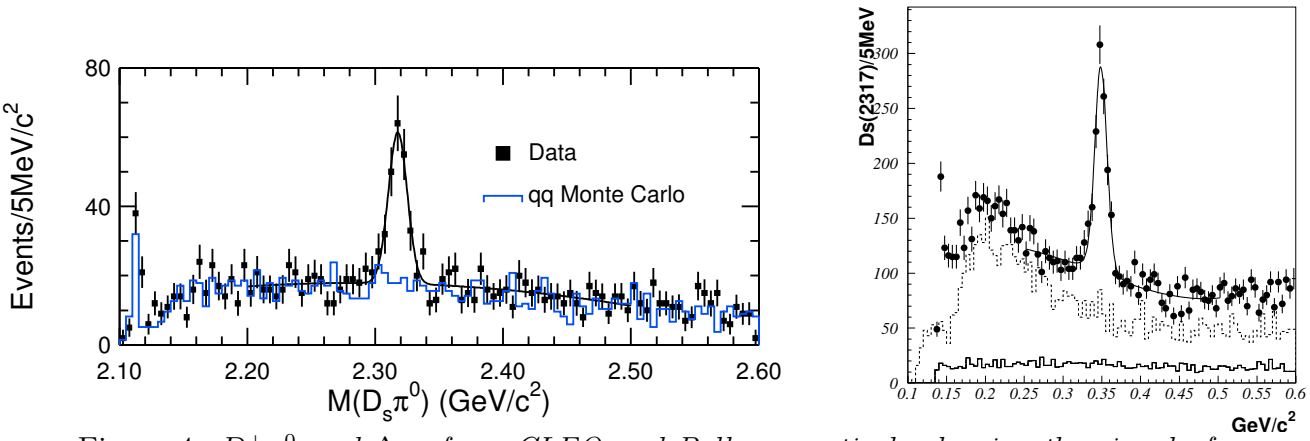

Figure 4: $D_s^+\pi^0$ *and* Δm *from CLEO and Belle respectively showing the signal of* $D_{sJ}^*(2317)^+$.

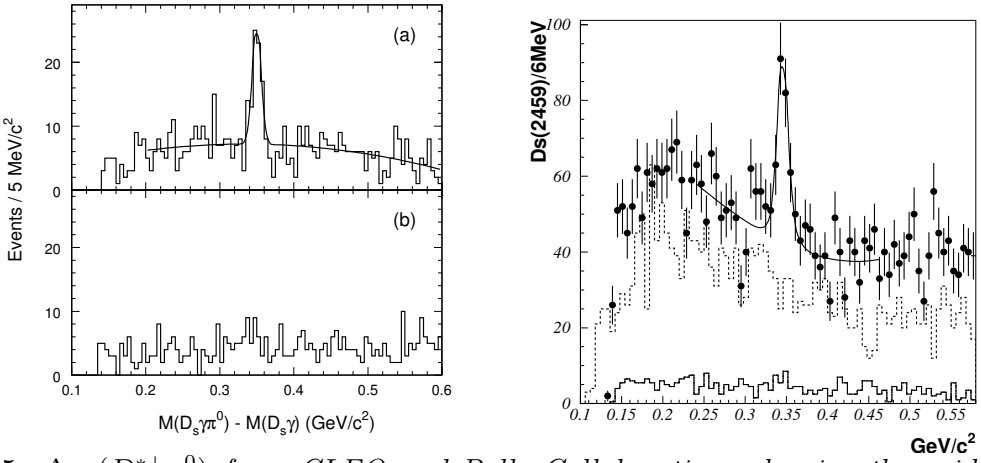

Figure 5: $\Delta m(D_s^{*+}\pi^0)$ *from CLEO and Belle Collaborations showing the evidence for* $D_{sJ}(2458)^+$. *Data are from continuum* e^+e^- *annihilations. The distribution from* D_s^{*+} *sidebands is also shown.*

No evidence has been found for narrow structures in $D_s^+\pi^\pm$ or $D_s^+\pi\pi$ final states.

5 The observation of $D_{sJ}(2458)^+$ by the *BABAR* experiment.

In order to study the $D_s^+\pi^0\gamma$ system, each D_s^+ candidate is combined with all combinations of accompanying π^0 candidates with momentum greater than 300 MeV/c and photon candidates of energy greater than 100 MeV/c^2. To suppress background, photon candidates that belong to any π^0 candidate are excluded and it is required that the combined momentum p^* in the e^+e^- center-of-mass mass frame of each $D_s^+\pi^0\gamma$ combination be greater than 3.5 GeV/c. The $D_s^+\pi^0\gamma$ invariant mass distribution is shown in Fig. 6. A small peak is observed near 2.46 GeV/c^2. The background underneath this peak is from several sources, which can be described in terms of mass differences defined as:

$$\Delta m(D_s^+\gamma) \equiv m(K^-K^+\pi^+\gamma) - m(K^-K^+\pi^+) \quad (1)$$

$$\Delta m(D_s^{*+}\pi^0) \equiv m(K^-K^+\pi^+\pi^0\gamma) - m(K^-K^+\pi^+\gamma)\,. \quad (2)$$

A scatter plot of these quantities is plotted in Fig. 6b. Two signals are clearly visible: $D_s^*(2112)^+ \to D_s^+\gamma$ decay combined with unassociated π^0 candidates, which appears as a horizontal band, and $D_{sJ}^*(2317)^+ \to D_s^+\pi^0$ decay combined with unassociated γ candidates, which appears as a band that is almost vertical.

An enhancement is evident in the vicinity of the overlap of these two bands with a $D_s^+\pi^0\gamma$ mass near 2.46 GeV/c^2. The upper histogram of Fig. 6c shows events in the $D_s^*(2112)^+$ signal region, and the shaded histogram shows those in the two $D_s^*(2112)^+$ sidebands. One can conclude that a state with decay to $D_s^+\pi^0\gamma$ is seen to exist over a background from $D_{sJ}^*(2317)^+$ combined with a γ. This background is peaked at a mass slightly higher than the signal. In Fig. 6d the subtracted plot shows the narrow signal fitted to a Gaussian shape on a second order polynomial background at $\Delta m(D_s^+\gamma) = 346.2 \pm 0.9$ MeV/c^2 (statistical errors only).

The signal, which is labelled $D_{sJ}(2458)^+$, may decay either through $D_s^+\pi^0\gamma$, $D_s^*(2112)^+\pi^0$ or $D_{sJ}^*(2317)^+\gamma$. To disentangle these decay modes and extract the most information from the data, a binless-maximum likelihood fit to the $D_s^+\pi^0\gamma$ system has been developed. The fit determines a $D_{sJ}(2458)^+$ mass of (2458.0 ± 1.0) MeV/c^2 and a measured Gaussian width equal to (8.5 ± 1.0) MeV/c^2. This mass value (yielding $\Delta m = 345.6 \pm 1.0$ MeV/c^2) agrees with that obtained by BELLE but differs from that obtained by CLEO.

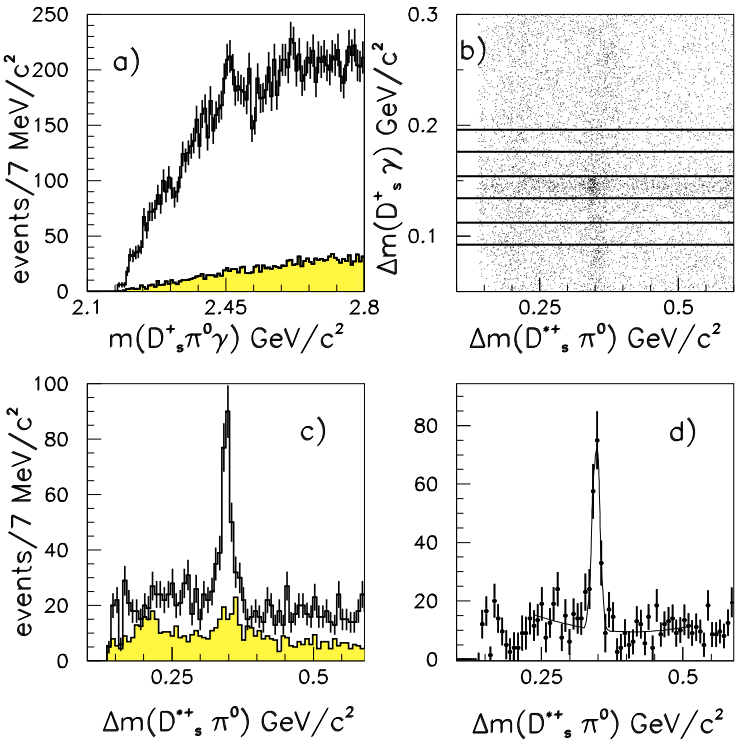

Figure 6: *BABAR* experiment. (a) The mass distribution for all selected $D_s^+\pi^0\gamma$ combinations. The shaded region is from D_s^+ sidebands defined by $1.912 < m(K^-K^+\pi^+) < 1.933$, $1.999 < m(K^-K^+\pi^+) < 2.020$ GeV/c^2. (b) The value of $\Delta m(D_s^+\gamma)$ versus $\Delta m(D_s^{*+}\pi^0)$ for all combinations. The horizontal lines delineate three ranges in $\Delta m(D_s^+\gamma)$. (c) The $\Delta m(D_s^{*+}\pi^0)$ mass distribution for the middle range of $\Delta m(D_s^+\gamma)$ (white) and for the upper and lower ranges (shaded). (d) The difference of the two histograms shown in (c). The curve is the fit described in the text.

The shape of the $D_s^+\pi^0$ and $D_s^+\gamma$ distributions in the $D_{sJ}(2458)^+$ mass region can be used in order to distinguish the two possible $D_{sJ}(2458)^+ \to D_s^*(2112)^+\pi^0$ and $D_{sJ}(2458)^+ \to D_{sJ}^*(2317)^+\gamma$ decay modes. These shapes are influenced by the allowed kinematic range for $D_{sJ}(2458)^+$ decay, as shown in Fig. 7a. Figs. 7b–7c show the $D_{sJ}(2458)^+$ background subtracted $D_s^+\pi^0$ and $D_s^+\gamma$ mass projections compared with MC simulations of the two hypotheses. The decay $D_{sJ}(2458)^+ \to D_s^*(2112)^+\pi^0$ is clearly favored.

The distribution of the angle ϑ_h of the decay $D_s^*(2112)^+ \to D_s^+\gamma$ in its center-of-mass with respect to the $D_{sJ}(2458)^+$ can be used investigate the spin-parity of the $D_{sJ}(2458)^+$. The resulting efficiency-corrected $\cos\vartheta_h$ distribution is

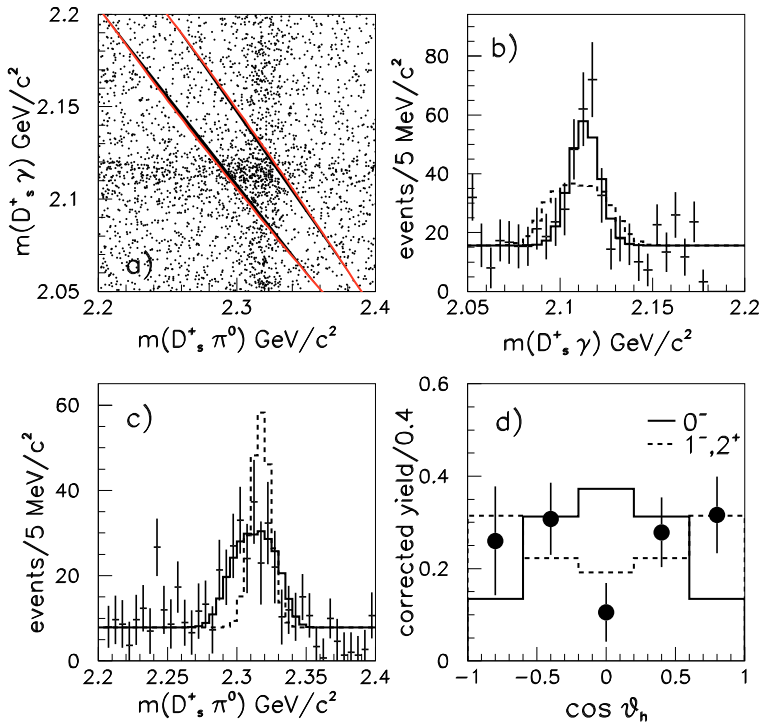

Figure 7: *BABAR* experiment. (a) The $D_s^+\pi^0$ versus $D_s^+\gamma$ mass distribution for all $D_s^+\pi^0\gamma$ combinations. The curves indicate the kinematically allowed region for $D_{sJ}(2458)^+$ decay. (b) Sideband subtracted $D_s^+\gamma$ mass distribution with (line) Monte Carlo simulation for $D_{sJ}(2458)^+ \to D_s^*(2112)^+\pi^0$ and (dashed) $D_{sJ}(2458)^+ \to D_{sJ}^*(2317)^+\gamma$. (c) A similar plot for the $D_s^+\pi^0$ mass distribution. (d) The efficiency corrected yield as a function of ϑ_h (statistical errors only). The solid (dashed) histogram corresponds to the best fit of a $\sin^2\vartheta_h$ $(1+\cos^2\vartheta_h)$ distribution.

shown in Fig. 7d (statistical errors only). This distribution is not consistent with a $\sin\vartheta_h$ distribution, which rules out a $D_{sJ}(2458)^+$ spin-parity assignment of $J^P = 0^-$.

MC simulations have been used to measure the detector resolution, leading to the conclusion that the intrinsic width of the $D_{sJ}(2458)^+$ is small ($\Gamma \lesssim 10$ MeV/c^2).

6 Conclusions

The decay of any $c\overline{s}$ state to $D_s^+\pi^0$ or $D_s^*(2112)^+\pi^0$ violates isospin conservation, thus guaranteeing a small width for these states. It is possible that the decays proceeds via $\eta - \pi^0$ mixing, as discussed by Cho and Wise [12].

The low mass and the absence of a $D_{sJ}^*(2317)^+ \to D_s^+\gamma$ favors $J^P = 0^+$ for $D_{sJ}^*(2317)^+$. The mass of $D_{sJ}^*(2317)^+$ lies below the DK threshold, the mass of $D_{sJ}(2458)^+$ lies above DK and below D^*K thresholds.

Different interpretations for these states have been proposed. In ref. [13, 14] models in terms of baryonia or molecules have been proposed. Ref. [15] provides an explanation in terms of relativistic vector and scalar exchange forces. Ref. [16] uses HQET plus chiral symmetry to predict parity doubling, i.e. the expectation is that the mass splitting between the 1^+ and 1^- states should be the same as for the 0^+ and 0^- states.

Since a $c\bar{s}$ mesons with these masses contradicts current models of charm meson spectroscopy [5, 6, 7], most likely these models need modification.

References

1. B. Aubert *et al*, Phys. Rev. Lett. **90**, 242001 (2003).
2. K. Hagiwara *et al*, (Particle Data Group) Phys. Rev. **D66**, 010001 (2001).
3. A. De Rujula, H. Georgi, and S.L. Glashow, Phys. Rev. Lett. **37**, 785 (1976).
4. N. Isgur and M. B. Wise, Phys. Rev. Lett. **66**, 1130 (1991).
5. S. Godfrey and R. Kokoski, Phys. Rev. **D43**, 1679 (1991).
6. S. Godfrey and N. Isgur, Phys. Rev. **D32**, 189 (1985).
7. M. Di Pierro and E. Eichten, Phy. Rev. **D64**, 114004 (2001).
8. B. Aubert *et al*, Nucl. Instrum. Meth. **A479**, 1 (2002).
9. D. Besson *et al* (CLEO Collaboration), hep-ex 0305100.
10. K. Abe *et al* (Belle Collaboration), hep-ex 0307041.
11. K. Abe *et al* (Belle Collaboration), hep-ex 0307052.
12. P.L. Cho and M.B. Wise, Phys. Rev. **D49**, 6228 (1994).
13. T. Barnes, F.E. Close and H.J. Lipkin, hep-ph/0305025.
14. E. van Beveren and G. Rupp, hep-ph/0305035.
15. R.N. Cahn and J.D. Jackson, hep-ph/0305012
16. W.A. Bardeen, E.Eichten and C.T. Hill, hep-ph/0305049.